CHAPTER 5

STUDY OF COLD COLLISIONS

This chapter reports the result of a study about collisions between two cold ^{85}Rb atoms under an influence of a light field. The experiment began with preparing cold atoms via MOT and loading them into an optical dipole trap (FORT) through cMOT and optical molasses as detailed in the previous chapter. A collision light pulse was applied to kick out atoms until only two were left in the trap. Preparation of only two atoms in FORT allowed us to observe the two-body collisions that were induced by the light. The cold collisions involving both the red- and blue-detuned light were studied as presented below in Section 5.1 and Section 5.2 respectively.

5.1 Cold collisions induced by red-detuned light

This section introduces a method to measure the time evolution of two atoms confined in an optical dipole trap (Section 5.1.1). This allowed us to detect the effects of (1) the red-detuned light on the decay rate for the probability of detecting two atoms and (2) the growth rates of the probabilities of detecting one and zero atoms in the trap. As a result, the probability of a single atom loss event for a two-body-collision loss, $P(1|2)$ was determined. To enhance this number and the single atom loading efficiency, specifically designed light pulses was introduce to prepare a single atom in the trap (Section 5.1.2).

5.1.1 Time evolution of two atoms

Firstly, the system consisting of only two atoms in the red-detuned collision light field is considered. When the atoms move toward each other in the ground state $|S+S\rangle$ and pass through the Condon point R_c where the light field is resonant with the transition, they have a probability to absorb a photon and be excited into the attractive excited state $|S+P\rangle$. This process is the first step of the FCC and RE processes that may lead to the trap loss as described before in Section 2.2. Here, the RE, which has more probability to occur, is in focus.

In order to study the parameters of the red detuned light that affect the cold collisions, the experiment began with loading two atoms into the FORT as previously mentioned in Section 4.1.3. An application of 10-ms imaging pulses identified the existence of the two atoms in the trap as illustrated in the first frame of Figure 5.1. In the second frame of the figure, the collision light pulse was applied for a duration of Δt to induce collisions between the atoms. As a result of these collisions, the atoms may gain enough energy to escape the trap. Finally, the number of atoms was counted again by the imaging pulse as shown in the last frame of Figure 5.1. The duration of Δt was varied for monitoring the time evolution of the pair. For each Δt, the experiment was repeated for 600 runs. Only the runs with a pair of atoms in the first imaging stage were counted. This corresponds to about 180 pairs of atoms measured in the first imaging stage. For each of the runs, the observed atom number in the last imaging stage could be two, one or zero as the result of none, single-atom or pair lost respectively. The probabilities to find two, one and zero atoms remaining

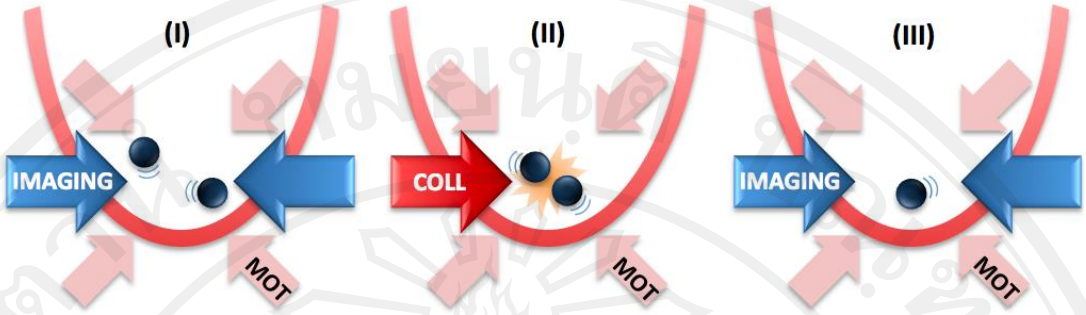

Figure 5.1 A sequence of the time evolution measurement of atoms in the FORT.

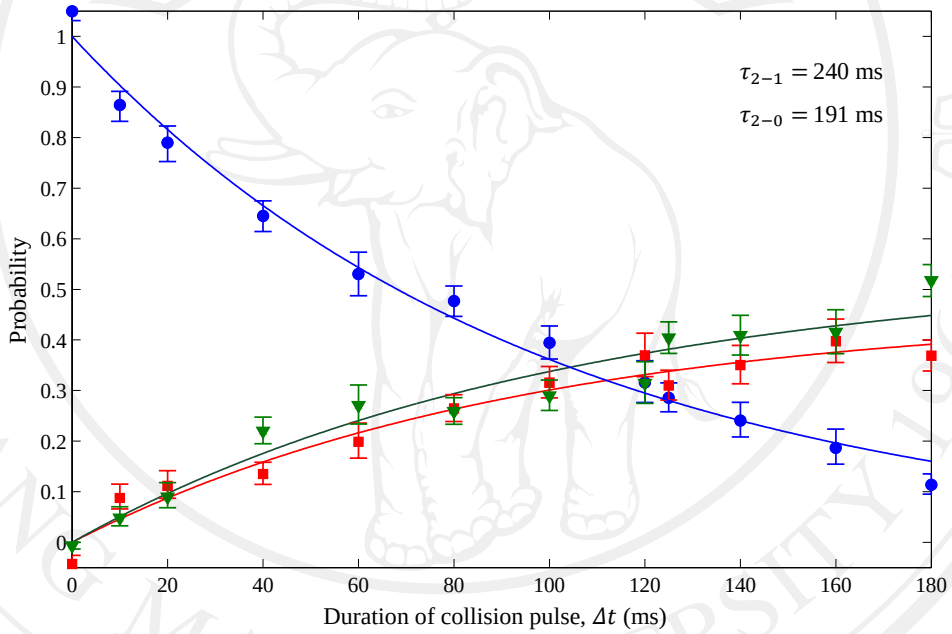

Figure 5.2. Probability to observe zero, one and two atoms in the FORT under the influence of a collision light pulse plotted as a function of the pulse duration $\boldsymbol{\Delta t}$. The blue circles indicate the survival probability of the pair. The red squares and the green triangles indicate the probability of obtaining one and zero atoms respectively. The solid lines indicate the curves fitted to the corresponding data by using a simple decay model that give us $\boldsymbol{P(1|2)}$ = 0.44. The parameters for the collision light pulse are $\boldsymbol{P_{col}}$ = 350 nW, $\boldsymbol{\delta_{col}}$ = −45 MHz, $\boldsymbol{P_{rep}}$ = 200 $\boldsymbol{\mu}$W and $\boldsymbol{\delta_{rep}}$ = −4.3 MHz.

in the trap were plotted as a function of Δt to show the time evolution of the trapped atoms as the result of a light-assisted collisions.

The atomic-pair evolution is shown in Figure 5.2. The blue circles indicate the survival probability of the pair after the collision light pulse was applied for Δt. As seen in the figure, the probability was decayed due to the atomic loss. At the same time, the probabilities to find one and zero atoms remaining in the trap were accumulated as represented by the red squares and green triangles respectively. In this case, the collision light pulse consisted of the collision beam and the cooling/repumping beams. The collision beam had a power, P_{col}, of 350 nW and its frequency was red detuned by 45 MHz from the D1 $F = 2$ to $F' = 3$ transition at the center of the trap (δ_{col} = -45 MHz). The cooling/repumping beams had a power, P_{rep}, of 200 μW and there frequency were red detuned by 4.3 MHz from the D2 $F = 3$ to $F' = 3$ transition at the center of the trap ($\delta_{rep} = -4.3$ MHz).

To extract the probability of the single atom loss event in these two-body collisions, the resulting data in the figure are fitted with a simple decay model of the pair probability. Let assume that the pair in the trap can decay to either one or zero atoms with a rate of $\frac{1}{\tau_{2-1}}$ or $\frac{1}{\tau_{2-0}}$ respectively due to the collisions. Here, τ_{2-1} and τ_{2-0} are the lifetime of the pair due to the single atom and pair collisional loss respectively. Moreover, the pair also decays because of the finite trapping lifetime of atoms, τ due to the background gas. In summary, the rate equations for the probability of the pair P_2 and the probability of single atom P_1 can be written as

$$\frac{\mathrm{d}P_2}{\mathrm{d}t} = -P_2\left(\frac{1}{\tau_2} + \frac{2}{\tau}\right), \tag{5.1}$$

$$\frac{\mathrm{d}P_1}{\mathrm{d}t} = P_2\left(\frac{1}{\tau_{2-1}} + \frac{2}{\tau}\right) - \frac{P_1}{\tau}. \tag{5.2}$$

where $\frac{1}{\tau_2} = \frac{1}{\tau_{2-1}} + \frac{1}{\tau_{2-0}}$. The solutions of the rate equations give us the probabilities of the pair, one and zero atoms as a function of time, which are

$$P_2(t) = P_2(0)\exp\left(-t\left(\frac{1}{\tau_2} + \frac{2}{\tau}\right)\right), \tag{5.3}$$

$$P_1(t) = P_2(0)\left(\frac{1}{\tau_{2-1}} + \frac{2}{\tau}\right)\left(\frac{\tau\tau_2}{\tau + \tau_2}\right)\left\{1 - \exp\left(-t\left(\frac{1}{\tau} + \frac{1}{\tau_2}\right)\right)\right\}\exp\left(-\frac{t}{\tau}\right), \tag{5.4}$$

$$P_0(t) = 1 - \big(P_2(t) + P_1(t)\big). \tag{5.5}$$

The solid lines in Figure 5.2 indicate the fitting curve of the observed data with the equations (**5.3**) - (**5.5**). The values of τ_{2-1} and τ_{2-0} are extracted as the fitting parameters. The probability of the single atom loss event from the collisions, $P(1|2)$ is defined by

$$P(1|2) = \frac{\tau_2}{\tau_{2-1}}. \tag{5.6}$$

From the fitting, τ_{2-1} and τ_{2-0} are equal to 240 ms and 191 ms respectively where the measured τ in this case is equal to 6.5 s. In this case, the calculated $P(1|2)$ is 0.44. The non-zero value of $P(1|2)$ represents the probability that the red detuned light induced collisions can contribute a single atom lost from the two-body collisions as well.

As a portion of the collision light pulse was for cooling atoms, the pair evolution under the influence of the cooling beams was investigated. To do this, the

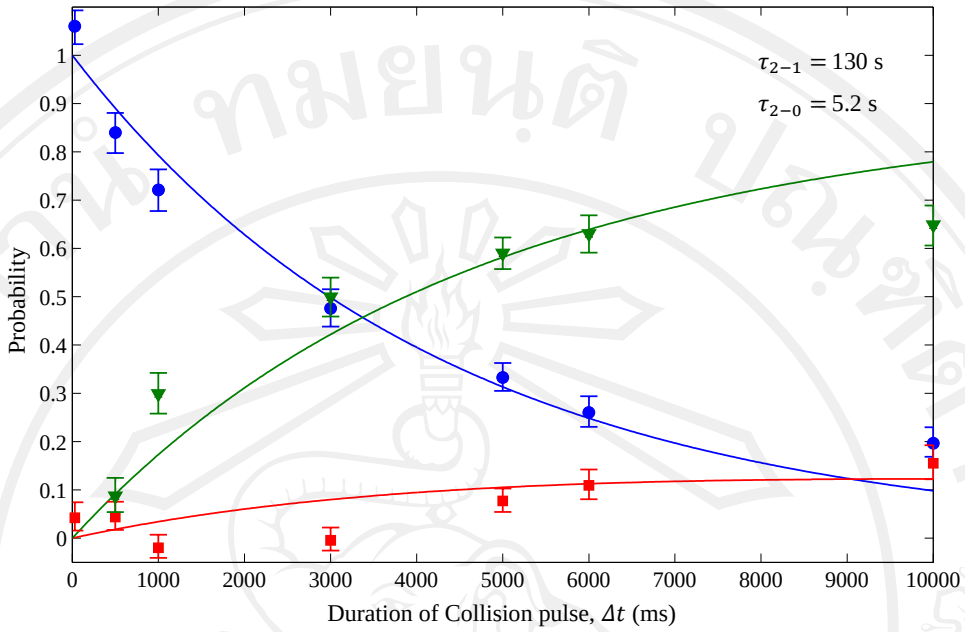

Figure 5.3. Probabilities of observing zero, one and two atoms in the FORT purely under the influence of the cooling/repumping light pulse. The probabilities are plotted as a function of the duration of the pulse. From the fit, $\boldsymbol{P(1|2)}$ is determined to be 0.04.

collision light pulse (in the second flame of Figure 5.1) consisted purely of the cooling beams with $P_{rep} = 0.64$ mW and $\delta_{rep} = -4.3$ MHz were used. The resulting evolution is shown in Figure 5.3. From the fit of the observed data, τ_{2-1} and τ_{2-0} are equal to 130 s and 5.2 s respectively. The obtained $P(1|2)$ was then only 0.04. This represents that most of the collisional losses induced by the cooling beams were the pair losses. The reason was that even though the beams were slightly red detuned from the D2 $F = 3$ to $F' = 3$ transition, they were red detuned by ~3 GHz from the D2 $F = 2$ to $F' = 1, 2, 3$ transitions as well. As a consequence, the atoms in the ground state with $F = 3$ were optically pumped into the other ground state efficiently by the near resonance beams. It was reasonable to assume that all collisions occurred

while the atoms were being in the $F = 2$ ground state and they experienced the beams with the detuning of –3 GHz. For this reason, the collisions contributed only the pair loss as a result of the large detuning (more detail is provided later in the subsection "Effect of the collision beam detuning").

In the case that the collision light pulse consisted of both the collision beam and the cooling beams, the results were assumed that only the collision beam to contributed the atomic loss, i.e. the measured collisional pair decay time τ_2 induced by the cooling beams was very long (more than 5 s) compared to τ_2 induced by the collision beam (~100 ms). This assumption was considered in all the results in the entire study.

Simulation of the red detuned light induced collisions

To understand the red detuned light assisted collisions between two cold atoms, the dynamic of the two atoms undergoing subsequent collisions are simulated. The model of this simulation relied on semiclassical GP and JV models detailed in Section 2.2.2. In the model used in this thesis, the three steps of the collision process are described by the quasimolecular state picture. Step I, two atoms in the ground state $|S + S\rangle$ approach each other. At the Condon point ($R = R_c$), the atoms may absorb a photon and transition to the excited state $|S + P\rangle$. Step II, in this $|S + P\rangle$, the atoms are accelerated toward each other as a result of the attractive excited-state energy, $U_e(R)$. Step III, the atoms decay to $|S + S\rangle$ by spontaneously emitting photon at the separation of R_s and gain a released energy E_r, which was equal to $U_e(R_c) - U_e(R_s)$.

The atoms share the energy E_r depending on their initial momentums. The atoms, of which the kinetic energy is higher than the trap depth, will escape the trap.

To simulate the collision process, the model begins with simulating two atoms in the optical dipole potential. Their spatial and velocity distributions follow the Maxwell-Boltzmann statistics; the initial positions of both atoms are randomly selected from the Maxwell- Boltzmann distribution, which depends on the trapping potential $U(x, y, z)$ and an initial temperature T of the atomic ensemble. The initial velocities are chosen randomly from the Gaussian (normal) distribution where the standard deviation $\sigma = \sqrt{k_B T/m}$ and m is the mass of the atoms.

The simulated atoms move under the trap confining force and are cooled by the Doppler cooling model. To make the atoms experienced the same cooling effect as in the experiment, the cooling rate of the experiment was measured from the ensemble temperature as a function of the cooling time. To do that, a single atom was prepared in the trap with temperature of 204 μK as reported in Section 4.2.2. Next, the atom was heated up to above 500 μK by turning off the dipole trap and turning on the blue detuned MOT cooling and repump beams at the same duration for 8 μs. After that the trap was turned back on to recapture the heated atom. With this heating method, the temperature of the atom could be as high as 967 μK as shown in Figure 5.4. After the heating process, the collision light pulse was introduced to the heated atom for the duration of Δt. Then the temperature was measured. The parameters of the pulse were $P_{col} = 350$ nW, $\delta_{col} = -45$ MHz, $P_{rep} = 350$ μW and $\delta_{rep} = -4.3$ MHz. As shown in Figure 5.5, the measured temperature (the blue circles in the figure) is plotted as a function of cooling time Δt. Finally, the Doppler cooling model

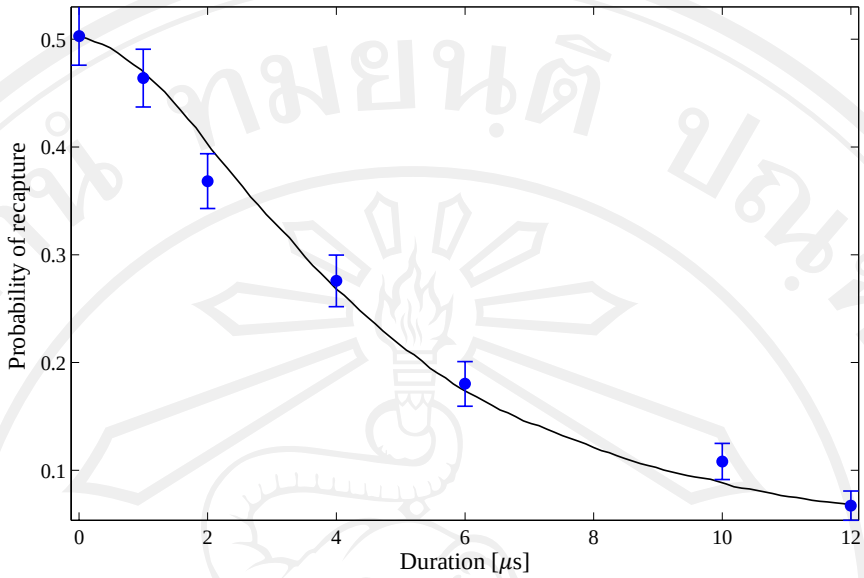

Figure 5.4 Probability to recapture a single atom plotted as a function of a duration that the atom get release from the trap, for the temperature measurement. The solid line is a fit of the experimental data giving the temperature of 967 ± 23 $\boldsymbol{\mu}$K.

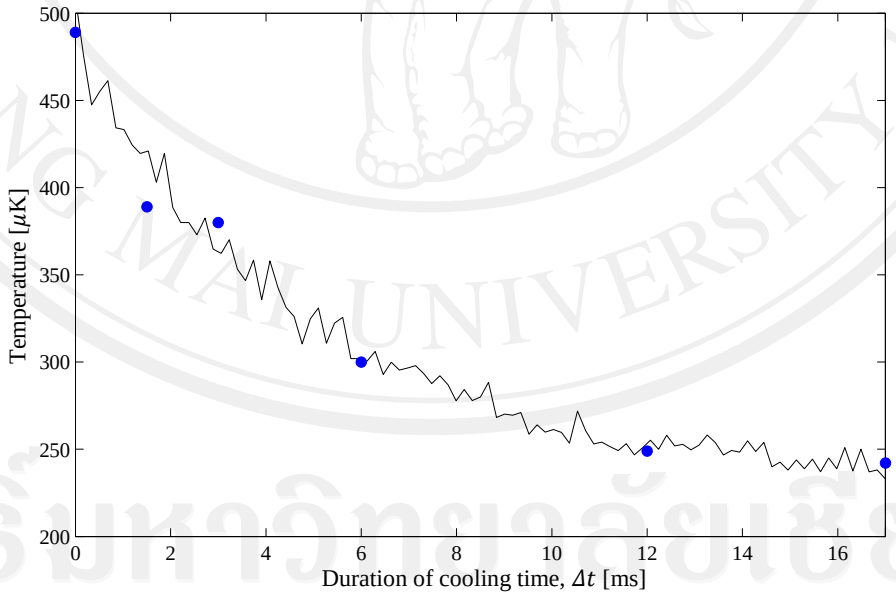

Figure 5.5. Temperature of a single atom plotted as a function of the cooling time of $\boldsymbol{\Delta t}$. The blue circles show the measured temperature and the solid line is from the simulation.

in the simulation was created in such the way that the simulation reproduced the observed time evolution as shown by the solid line in the figure.

For a simulation involving two atoms travelling in the trapping potential and being cooled by the Doppler cooling, they may move toward each other and get excited by absorbing a photon in the collision beam at R_c. The excitation probability is determined by the Landau-Zener (LZ) formalism in dressed state picture as shown in Figure 5.6 (a). Previously in Section 2.2.1, the attractive excited-state potential for the long-rang internuclear separation R is approximated to be $U_e(R) = \frac{C_3}{R^3} + \hbar\omega_0$, where $C_3 = -20.13$ a.u. [52]. The ground state is assumed to be independent of R. For the dressed-state picture, the energy level of the excited state is offset by the photon energy. It seems that to cross the energy level of the ground state at R_c as shown by the dotted line in Figure 5.6 (a) but it really does not as shown by the solid line.

The two atoms, which are approaching each other, have a probability of P_{LZ} in equation (2.24) to undergo the LZ transition to the other dressed state when they are passing R_c (dotted line in Figure 5.6 (a)). The atoms can move adiabatically through this region as well with the probability of P_A in equation (2.25) and end on the excited state potential as represented with the green arrow. If the atoms pass though the region by the LZ transition path, they will reach R_c again when they move away form each other (see the orange arrow). In this case, they may move adiabatically following the upper dressed state. The atoms will be attracted to approach each other and return back to R_c again. At this point, the atoms may undergo the LZ transition to the other dressed state and end on the excited state potential. If not, this scenario will

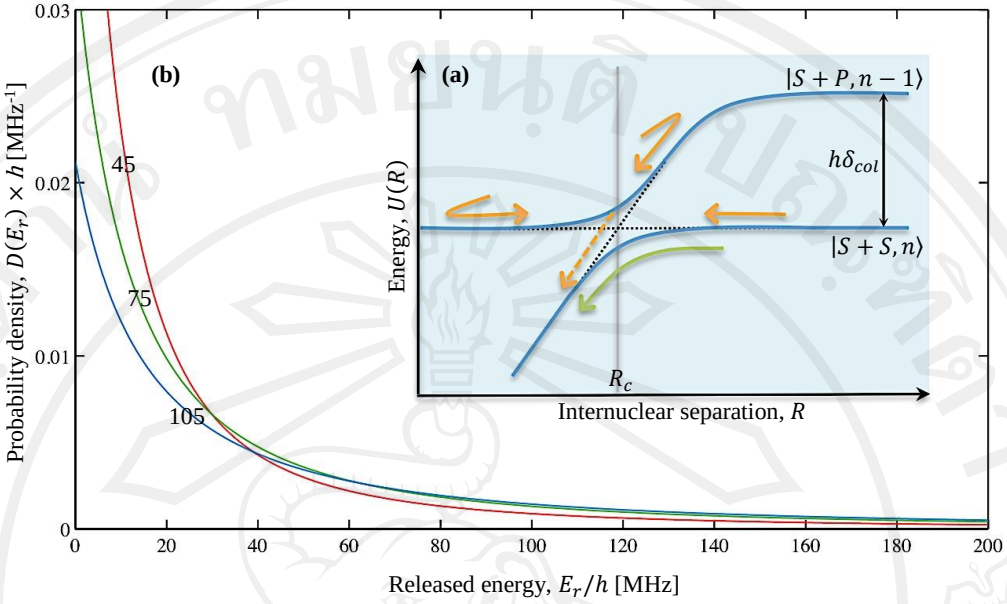

Figure 5.6. (a) Dressed state picture showing an avoided crossing between $|\boldsymbol{S+S,n}\rangle$ and $|\boldsymbol{S+P,n-1}\rangle$ at $\boldsymbol{R_c}$. (b) Probability density of the released energy for $\boldsymbol{v(R_c)} =$ 0.2 ms^{-1} for three different values of $\boldsymbol{\delta_{col}}$ (45, 75, and 105 MHz).

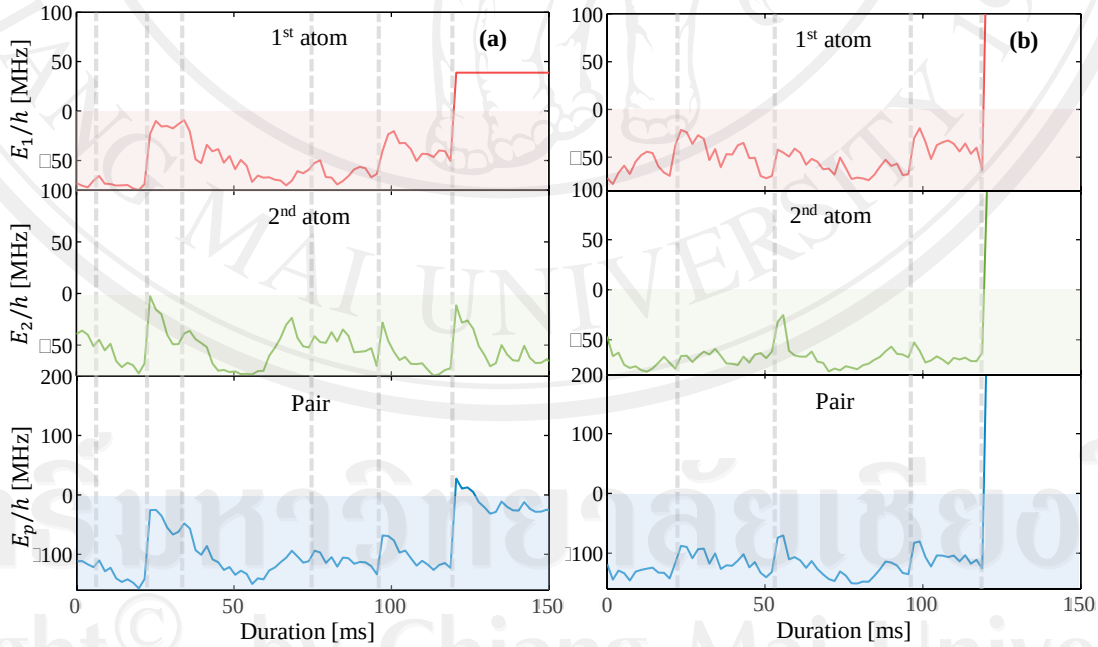

Figure 5.7 The total energies of individual atoms and of the pair as a function of the collision duration. The simulation ends with single atoms loss (a) and the other ends with the pair loss (b). The dashed lines indicate when the collisions happen.

repeat itself. From these processes, the probability that the atoms are in the excited state at the end, can be written as:

$$P_e = P_A + \frac{P_{LZ}^2 P_A}{1 - P_A^2}. \tag{5.7}$$

This P_e is used in the simulation as the excitation probability of the mutually approaching atoms at R_c that is step I of the collisional model.

In step II, the atoms are accelerated radially along the internuclear separation by $U_e(R)$. From equation (2.19), their radial velocity can be given by

$$v(R) = \sqrt{v(R_c)^2 - \frac{2}{\mu}[U_e'(R) - U_e'(R_c)]}, \tag{5.8}$$

where $U_e'(R)$ is $U_e(R)$ plus a centrifugal barrier. Due to the decay of the atoms in the excited state with the rate Γ_M, the survival probability of the atoms in the excited state traveling from R_c to R_s can be written as

$$S(R_s) = \exp\left(-\Gamma_M \int_{R_c}^{R_s} \sqrt{v(R_c)^2 - \frac{2}{\mu}[U_e'(R) - U_e'(R_c)]}\right). \tag{5.9}$$

As the separation where the atoms decayed is predicted from the equation above, the energy $E_r = U_e(R_c) - U(R_s)$ released in step III of collision is determined. Figure 5.6 (b) shows examples of the probability densities of the released energy $D(E_r)$ for three values of δ_{col} which are -45, -75, and -105 MHz where $v(R_c) = 0.2$ m/s. As seen in the figure, the excited atoms had a high probability to release a small quantity of E_r during the collision. The predicted E_r is shared to both collision partners while the total momentum is conserved and the velocities of the atoms

change along their internuclear separation $\boldsymbol{R}$. The conditions for sharing E_r can be written as:

$$-\Delta \boldsymbol{v}_1 = \Delta \boldsymbol{v}_2 = -\alpha \boldsymbol{R}\,, \tag{5.10}$$

$$v_1^2 + v_2^2 + \frac{2E_r}{m} = v_1'^2 + v_2'^2. \tag{5.11}$$

Here $\boldsymbol{v}_1$and $\boldsymbol{v}_2$ are the velocity of the first and the second atoms before the collision respectively, $\boldsymbol{v}_1'$ and $\boldsymbol{v}_2'$ are the velocity of the first and second atoms after the collision respectively, $\Delta \boldsymbol{v}_i = \boldsymbol{v}_i' - \boldsymbol{v}_i$ where $i = 1$ or 2, the relative position vector $\boldsymbol{R} = \boldsymbol{R}_1 - \boldsymbol{R}_2$ where $\boldsymbol{R}_1$ and $\boldsymbol{R}_2$ are the position vectors of the first and second atoms respectively, and α is a positive constant. From the equations above, α could be determined by

$$\alpha = \frac{\boldsymbol{R}\cdot\boldsymbol{v} + \sqrt{\frac{4R^2E_r}{m} + (\boldsymbol{R}\cdot\boldsymbol{v})^2}}{2R^2}\,, \tag{5.12}$$

where the relative velocity $\boldsymbol{v} = \boldsymbol{v}_1 - \boldsymbol{v}_2$. After gaining energy from the collision, the atom, of which kinetic energy is larger than the trap depth, is determined to be lost. As a result, both single- and two-atom loss events can happen as shown in Figure 5.7 (a) and (b) respectively. The figure further shows the total energies of individual simulated atoms and their combined energy E_1, E_2 and $E_p = E_1 + E_2$ respectively as a function of time. The gray dashed lines indicate when the inelastic collisions occur. The simulation shows that most of the collisions release a low E_r, which is not high enough to yield any atoms lost. After a collision, the energy gained by each atom tends to dissipate away as a result of the Doppler cooling process. This scenario repeats itself until the collision releases high enough energy to make either one or two

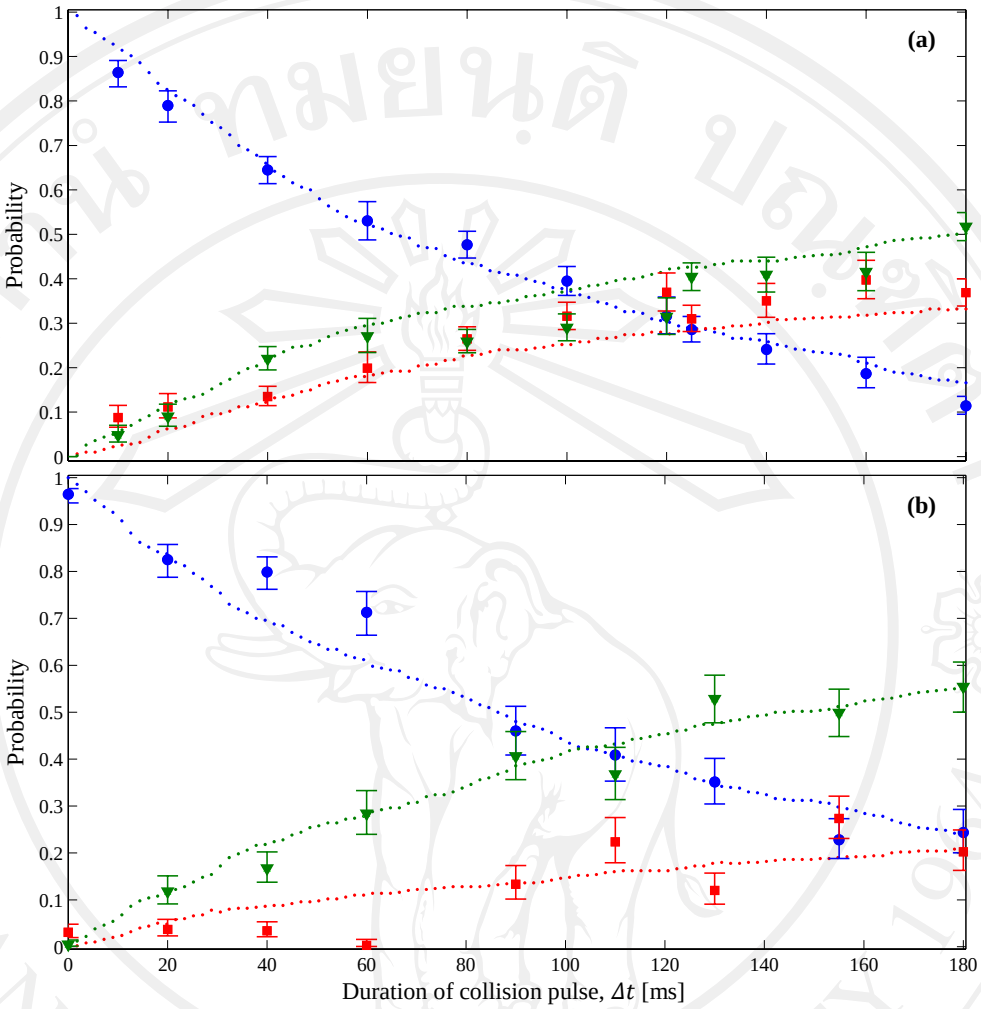

Figure 5.8 A atom pair's evolution for the cooling/repumping beam power of 200 μW in (a) and 350 μW in (b). The dotted lines indicate the result from simulations.

atoms lost. For a broad range of intermediate released energy, it is possible to lose only one of them due to the nonzero speed of the center of mass. For a large released energy, it has a high probability to lose both them. The programming code of this simulation is in Appendix B.

The simulation results (dotted lines) are plotted against with the experimental data as shown in Figure 5.8. For these results, the probabilities of the remaining two, one and zero atoms in the trap are calculated by averaging over 500 pairs of atoms.

The Rabi frequency Ω for the LZ transition is adjusted until the averaged decay time of the pairs is the same as that from the experiment in order to compensate for the simplicity imposed onto the simulation model. For the experimental result in figure (a), the collision light pulse consisted of the collision beam with $P_{col} = 350$ nW and $\delta_{col} =$ -45 MHz and the cooling/repump beams with $P_{rep} = 200\ \mu$W and $\delta_{rep} = -4.3$ MHz. In Figure 5.8 (b), all the beam parameters have the same values as in figure (a) except $P_{rep} = 350\ \mu$W. As seen in the figure, the simulation results agree well with the experiments.

Comparison between the pair evolutions in (a) and (b) shows that the cooling beams play a crucial role in the collision process. The result shows that $P(1|2)$ decreases when the power of the beams is increased. That is because higher power provides more efficient cooling mechanism. Consequently, the colliding pairs could

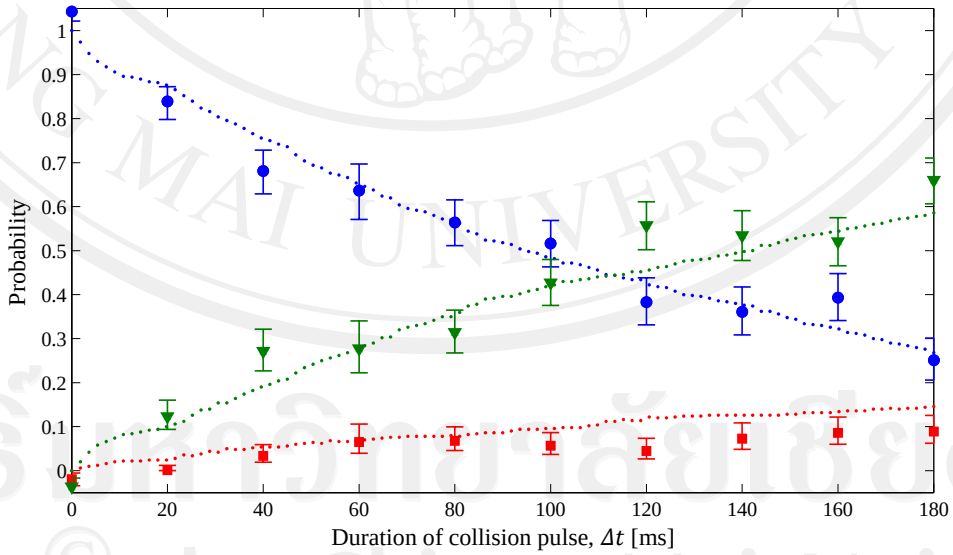

Figure 5.9. Probability to observe two, one and zero atoms in FORT under the influence of the collision light pulse plotted as a function of the pulse duration where $\boldsymbol{\delta_{col}} =$ -75 MHz.

have a lower E_P before collisions and they require higher E_r for the case of the single-atom loss. However, higher E_r has less possibility to be released. This leads to the reduction of $P(1|2)$.

The other detuning of collision beam, δ_{col} = -75 MHz, is simulated as well. As shown in Figure 5.9, the simulation agrees well with the experiment. In the experiment, the collision light pulse consisted of the collision beam with $P_{col} = 600$ nW and the cooling/repump beams with $P_{rep} = 400$ μW and $\delta_{rep} = -4.3$ MHz.

Effect of the collision beam detuning

As shown in Figure 5.6 (b), the probability distribution of the released energy E_r depends on the detuning of the collision beam δ_{col}. For the case of large detuning, the colliding atoms have more chance to release a large amount of energy compared with the small detuning. The reason is that at the corresponding Condon point R_c for the larger δ_{col}, the excited state potential has a higher gradient; the excited pair can go to the shorter range of its internuclear separation, in which case it gains a larger E_r. From this reason, $P(1|2)$ would depend strongly on δ_{col}.

The pair evolutions were observed for several values of δ_c (from –30 to –110 MHz) to study the effect of the detuning on the collisions. The other parameters of the collision pulse were fix as used in Figure 5.8 (a) except P_{col}. For each value of δ_c, P_{col} was adjusted such the way that the pair decay time was about 90 ms. The used P_{col} was plotted as a function of δ_c as shown in Figure 5.10 (b). The $P(1|2)$ value was extracted from each pair evolution and plotted against δ_c as shown in Figure 5.10

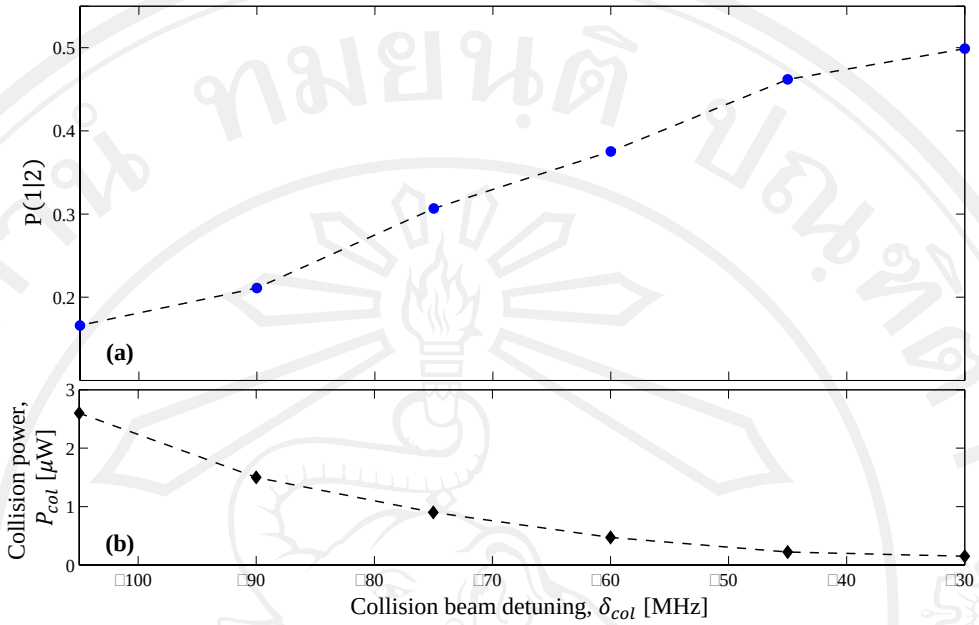

Figure 5.10. (a) P (1|2) extracted from the pairs evolution plotted as a function $\boldsymbol{\delta_{col}}$. (b) The used $\boldsymbol{P_{col}}$ for each value of $\boldsymbol{\delta_{col}}$.

(a). The resulting data reveal that all the obtained $P(1|2)$ values are more than zero. $P(1|2)$ rises obviously when δ_c is closely to the resonance. The highest observed value is equal to 0.5 at the detuning of –30 MHz. As a result of the nonzero $P(1|2)$ values, a use of the collision light pulse with these parameters to prepare single atoms provided the loading efficiency exceeding the 50% limit as reported in next section.

5.1.2 Single atom loading efficiency

To prepare a single atom by using the red detuned light assisted collisions, the experiment began with loading about 30 atoms into the FORT. The collisions between the atoms were induced by applying of the collision light pulse for 402 ms. This duration was optimized for getting the highest probability of loading a single

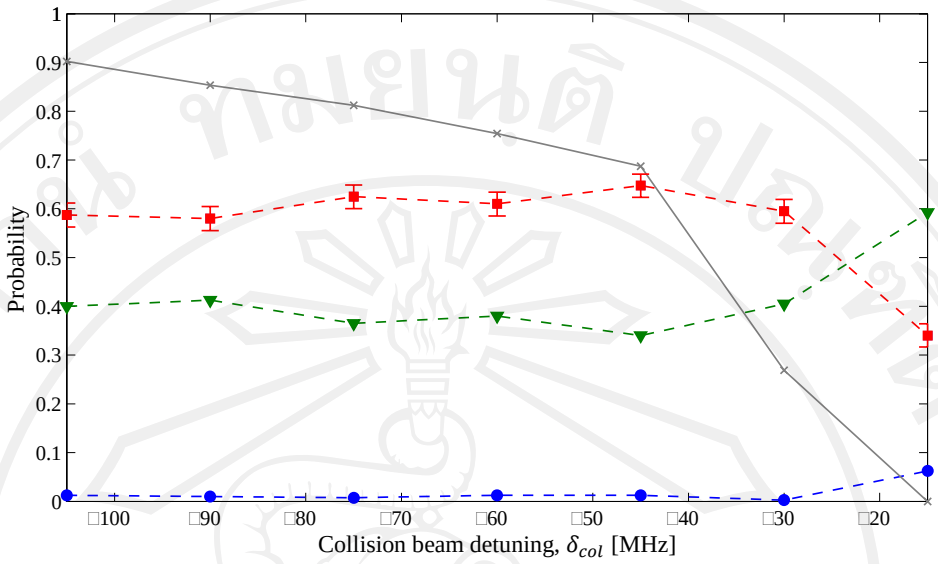

Figure 5.11. Single atom loading probability as a function of $\boldsymbol{\delta_{col}}$. Blue circles, red squares and green triangles indicate the probability of obtaining two, one and zero atoms respectively. The black crosses represent a single atom survival probability after a collision pulse of 1.5 s.

atom and the lowest probability of loading two. After the collision duration, an application of imaging pulse counted the number of atoms (see the details in Section 4.2.1). These processes were repeated for 400 times for determining the probabilities of loading zero, one and two atoms. The probabilities were plotted against δ_{col} as shown in Figure 5.11.

In order to understand the resulting efficiency of loading a single atom, a survival probability of an atom after the collision light pulse was applied for 1.5 s, was observed. The survival probability represented the trapping lifetime of an atom while the collision pulse was applied. If the survival probability was low, the lifetime was short.

In Figure 5.11, the trend of the single atom loading efficiency agrees well with the $P(1|2)$ values in Figure 5.10. However the single atom loading efficiencies for the small detuning (–30 and –15 MHz) are dropped, even though the $P(1|2)$ value is high. This would come from shorter trapping lifetime indicated by lower survival probability. As a compromise between $P(1|2)$ and the trapping lifetime, the collision light pulse with the detuning of –45 MHz could provide loading efficiency as high as 0.63.

The effect of the cooling/repumping-beam power P_{rep} on the single atom loading efficiency was investigated as well. To do that, single atoms were prepared by using the collision pulse with the same parameters in Figure 5.8 (a) except P_{rep}. The value of P_{rep} was varied from 50 to 550 μW. The observed loading efficiency is plotted as a function of P_{rep} as shown in Figure 5.12. In the low power regime, lower survival probability indicates shorter trapping lifetime. This leads to lower loading efficiency. The collision pulse with P_{rep} = 50 μW contributes the loading efficiency of only 0.39. This represents a lack of the cooling mechanism. When P_{rep} is higher, the loading efficiency increases. The rise in the loading efficiency continues until the beam power is more than 200 μW. The loading efficiency started to drop. That is because of the same reason as mentioned before in the comparison between the two pair evolutions involving $P_{rep} = 200$ and 350 μW in Figure 5.8.

With an application of the collision light pulse with the same parameters as used in Figure 5.8 (a) the single atom loading efficiency could be as high as 63%. This loading efficiency was represented by the largest peak of the histogram of the integrated fluorescence signal for the 1,000 experimental realizations in Figure 5.13.

The result shows that a use of the red-detuned light for preparing single atoms can provide the efficiency higher than the limit of 50% obviously.

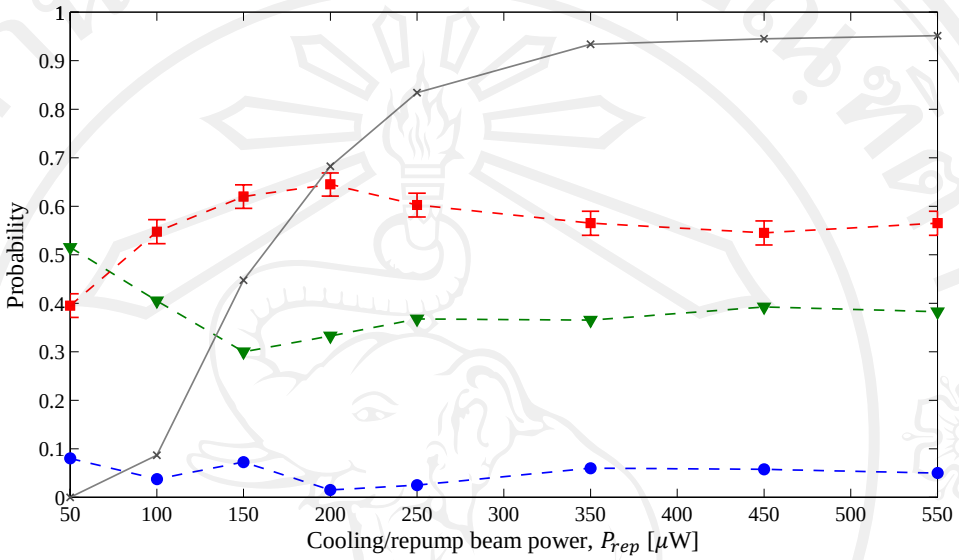

Figure 5.12. Single atom loading probability as a function of $\boldsymbol{P_{rep}}$. The symbols have the same meanings as in previous figure.

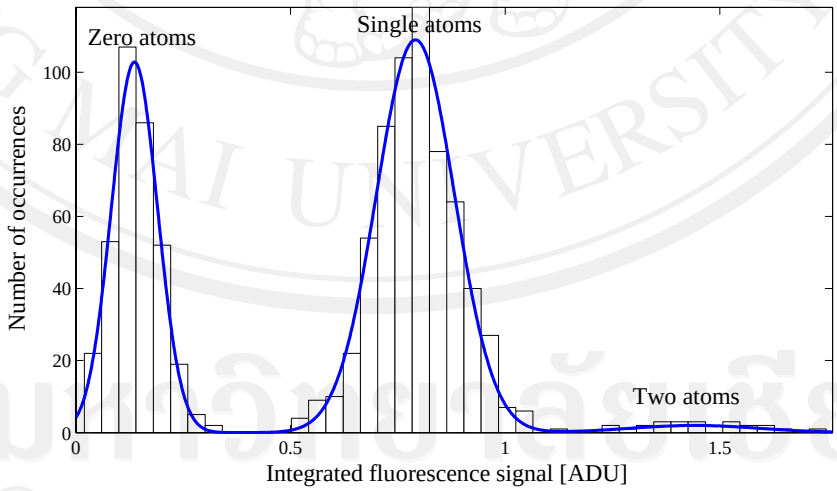

Figure 5.13. Histogram of the integrated fluorescence signal of each image for 1,000 realizations of the experiment. The largest peak represents the single atom loading probability of 63.00 ± 1.53%.

5.2 Cold collisions induced by blue detuned light

In this section, the cold collisions induced by the blue detuned light were studied. The experiment began with observing the time evolution of two atoms in the FORT as reported in Section 5.2.1. A simulation of two-body collisions was used to obtain the insight of the collisional processes. Finally, a collision light pulse was employed for loading a single atom in the FORT. The effect of the pulse parameters on the single atom loading efficiency was investigated to enhance the loading efficiency as presented in Section 5.2.2.

5.2.1 Time evolution of two atoms

Let consider the system of two atoms in the ground state $|S+S\rangle$ being exposed by the blue detuned light. A collision between the atoms begins with absorbing the photon at a separation of R_c. The atoms transition to the repulsive potential of $|S+P\rangle$. When the atoms move away from each other, they decay back to $|S+S\rangle$. Consequently, the atoms gain the energy of $\hbar\delta_{col}$ as detailed before in Chapter 2.

The collisional processes described above provide the capability to control the energy released from the collision by tuning the detuning of the light. If the energy is set equal to the trap depth, this would contribute a high value of $P(1|2)$. That is because the energy is enough for making only single atoms lost from the trap for the low-energy colliding pair. For this purpose, the pair evolution under the effect of blue detuned light was investigated. The collision light pulse consisted of the collision beam with $P_{col} = 11\ \mu$W and $\delta_{col} = 85$ MHz and the cooling/repump beams with

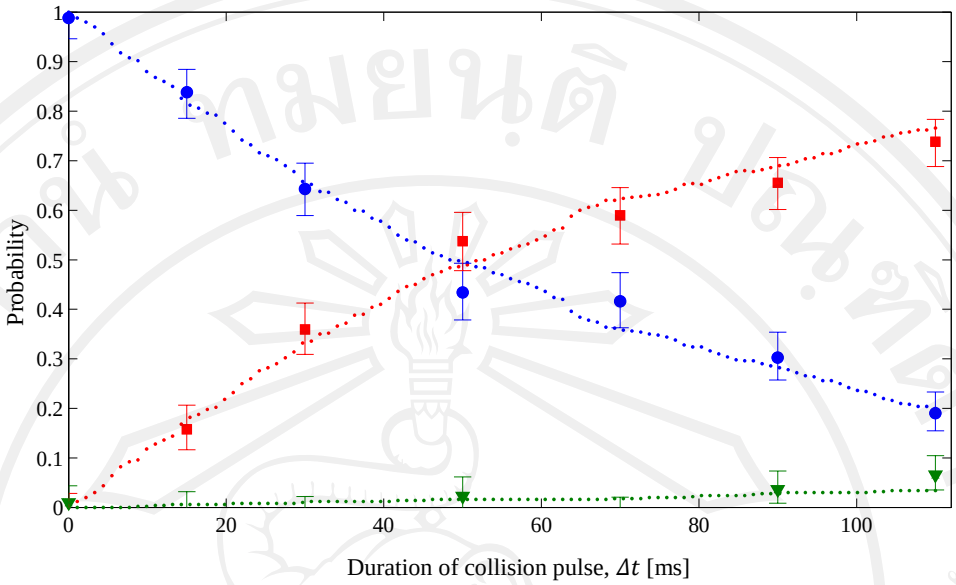

Figure 5.14. The pair evolution as a function of $\boldsymbol{\Delta t}$ for $\boldsymbol{\delta_{col}} = 85$ MHz.

$P_{rep} = 640\ \mu$W and $\delta_{rep} = -4.3$ MHz. As expected, the result in Figure 5.14 shows that the most occurrence of the collisions contributed only the single-atom loss as represented by the $P(1|2)$ value of 0.96.

The reason for obtaining the near deterministic $P(1|2)$ is discussed below. As the released energy was equal to the trap depth ($E_r = U_0$), the pair energy after collision could be written as $U_0 < E_p < 2U_0$ where the reference level is at the bottom of the trap. If both atoms had the total energy lower than U_0, neither atom escaped from the trap. The atoms with a mount of total energy were cooled down by the light pulse and might collide with each other again. This scenario was then repeated until one of them gained the most of E_r. In this case, the atom with total energy larger than U_0 would escape from the trap while the other still was confined in the trap. From this processes, the collisions induced by this light pulse contributed only a single-atom loss except for the collision between the high-energy atoms, of

which the probability to occur was very low. For getting the insight of these collisional processes, the dynamic of the colliding atoms was simulated to reproduce the observed pair evolution. The simulation result agrees well with the experiment as indicated by the dotted line in Figure 5.14. The detail of the simulation was explained below.

For the case of blue detuned light, the processes in the simulation are the same as in the case of red detuned light accept for some details as following. First, an excitation probability of the simulated atoms is different. To determine the excitation probability, the dressed state picture is considered. In Figure 5.15 the atoms, which are initially in $|S+S,n\rangle$ state may undergo an adiabatic passage followed by a LZ transition as indicated by the green arrows, or vice versa as indicated by the orange arrows. In both case, the atoms end at $|S+P,n-1\rangle$. The excitation probability can be calculated as

$$P_e = 2P_{LZ}(1-P_{LZ}). \tag{5.13}$$

Second, the energy release E_r in this collision process is fix as the constant value of $\hbar\delta_{col}$. The last, the momentum of individual atoms changes in opposite direction compared with the case of the red detuned light due to the repulsive force. So we can rewrite Equation (**5.10**) as

$$\Delta\boldsymbol{v}_1 = -\Delta\boldsymbol{v}_2 = \alpha\boldsymbol{R}\,. \tag{5.14}$$

We get a new value of α by

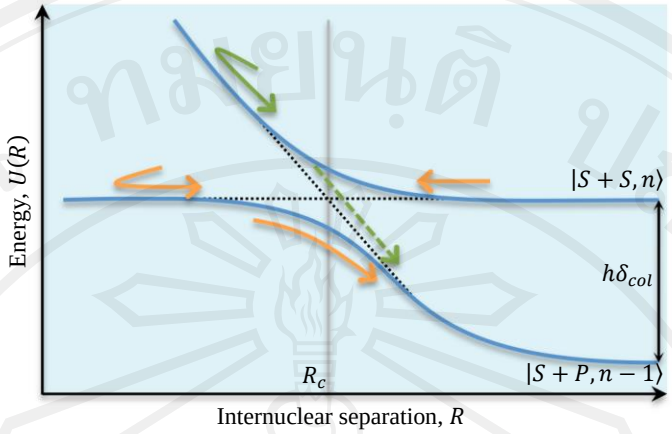

Figure 5.15. Dressed state picture showing an avoided crossing between two quasimolecular states around $\boldsymbol{R_c}$. The color arrows show the different excitation paths.

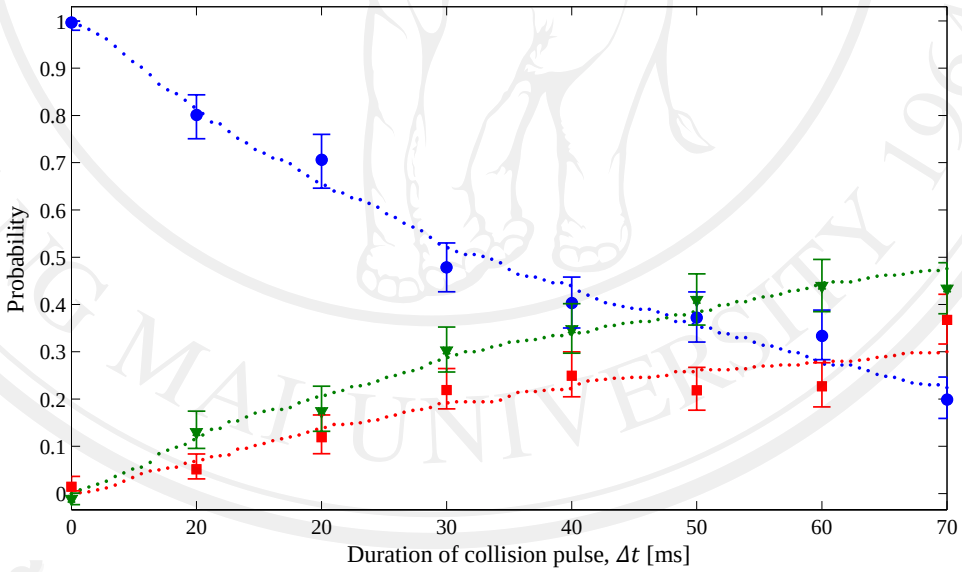

Figure 5.16. The pair evolution as a function of the duration $\boldsymbol{\Delta t}$ for the case of $\boldsymbol{\delta_{col}} = 185$ MHz.

$$\alpha = \frac{-\boldsymbol{R}\cdot\boldsymbol{v} + \sqrt{\frac{4R^2E_r}{m} + (\boldsymbol{R}\cdot\boldsymbol{v})^2}}{2R^2}. \qquad (5.15)$$

The pair evolution under the influence of the light with the detuning of 185 MHz was observed as well. In this measurement, the collision light pulse consisted of the collision beam with $P_{col} = 7\ \mu$W and the cooling/repump beams with $P_{rep} = 640\ \mu$W and $\delta_{rep} = -4.3$ MHz. The experimental and simulation results were plotted in Figure 5.16. The result gave us $P(1|2) = 0.33$, which was much lower than the previous case. The significant reduction of $P(1|2)$ for a high detuning was come from the high released energy, which was more than twice of the trap depth. This amount of energy was high enough to make both of atoms lost from the trap.

5.2.2 Deterministic preparation of single atoms

The effect of the parameters of the collision light pulse on the single atoms loading efficiency is explored in this section. The parameters studied were the collision beam detuning δ_{col}, the collision beam power P_{col} and the cooling/repump power P_{rep}. Let consider first the δ_{col}, which is used for determining the released energy.

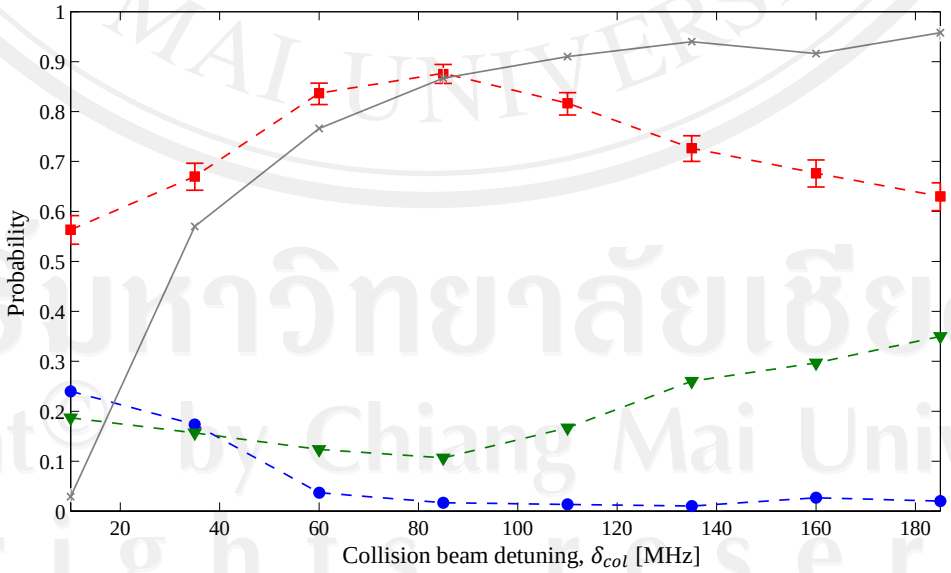

Figure 5.17. Single atom loading efficiency plotted as a function of $\boldsymbol{\delta_{col}}$.

In the measurement, the cooling/repump beam parameters and the duration were fixed at the same values used in Figure 5.14. For each detuning of the collision beam, the beam power was adjusted for maximizing the loading efficiency. The single atom loading efficiency is plotted as a function of δ_{col} as represented by the red squares in Figure 5.17. The black crosses indicate the single atom survival probability after the collision pulse of 3.5 s that is used for estimating the trapping lifetime of single atom.

The loading efficiency was highest when the δ_{col} was equal to 85 MHz corresponding with the trap depth. This agrees well with the $P(1|2)$ observed before. For the other detunings, the efficiency dropped for both smaller and larger detuning. When the detuning was closed to the atomic resonance, the trapping lifetime of single atom decreased. This suppressed the loading efficiency. When the detuning was above 85 MHz, the released energy was higher than the trap depth. Even though the trapping lifetime was longer, but the excess energy leaded to the two-atom loss. This agrees well with the $P(1|2)$ observed before in the case of 185-MHz detuning.

The effect of the collision beam power on the loading efficiency was shown in Figure 5.1 (a). The single atom loading efficiency was plotted as a function of P_{col} along the probabilities of loading zero and two atoms. In the measurement, the cooling/repump-beam parameters and the collision-beam detuning were fixed at the same values used in Figure 5.14. For each value of P_{col}, the duration of the pulse was adjusted to get the maximum loading of one atom at the end of the pulse. The used duration as a function of P_{col} is shown in Figure 5.18 (b). The black crosses in the figure (a) indicate the survival probability after a collision pulse of 3.5 s.

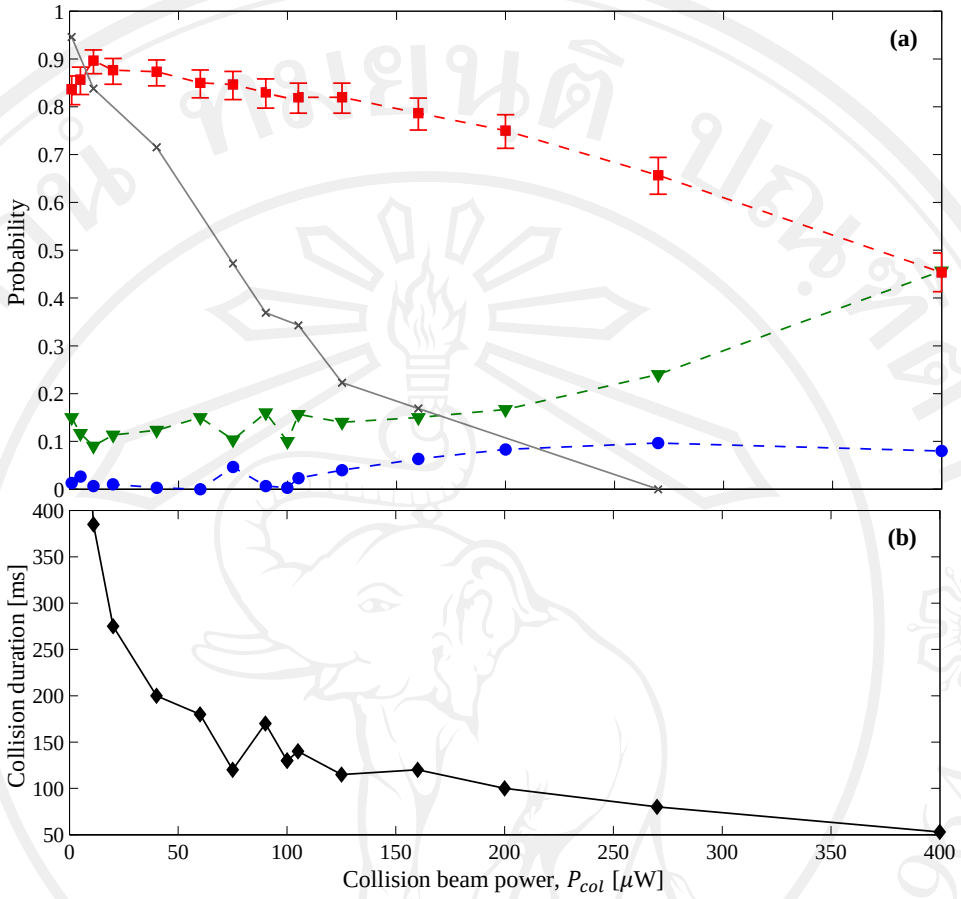

Figure 5.18. (a) Single atom loading probability as a function of $\boldsymbol{P_{col}}$. (b) The collision duration was adjusted for each $\boldsymbol{P_{col}}$. The duration used for $\boldsymbol{P_{col}} = 1\ \boldsymbol{\mu}$W which is equal to 2750 ms is not shown.

In the figure (a), the result shows that the loading efficiency is highest at the P_{col} of 11 μW and the collision duration of 385 ms (the same values as used in Figure 5.14). When P_{col} is lower than 11 μW, the trapping lifetime was longer as represented by the survival probability. However, the efficiency drops down because the used collision duration is too long. For example, in the case of P_{col} = 1 μW, the duration is 2.75 s. This duration is comparable with the measured pair-decay time of ~ 4 s due to the cooling/repump beams (in Figure 5.3). During the collision duration, the red-detuned cooling/repump beams induced the pair loss that disturbed the load of

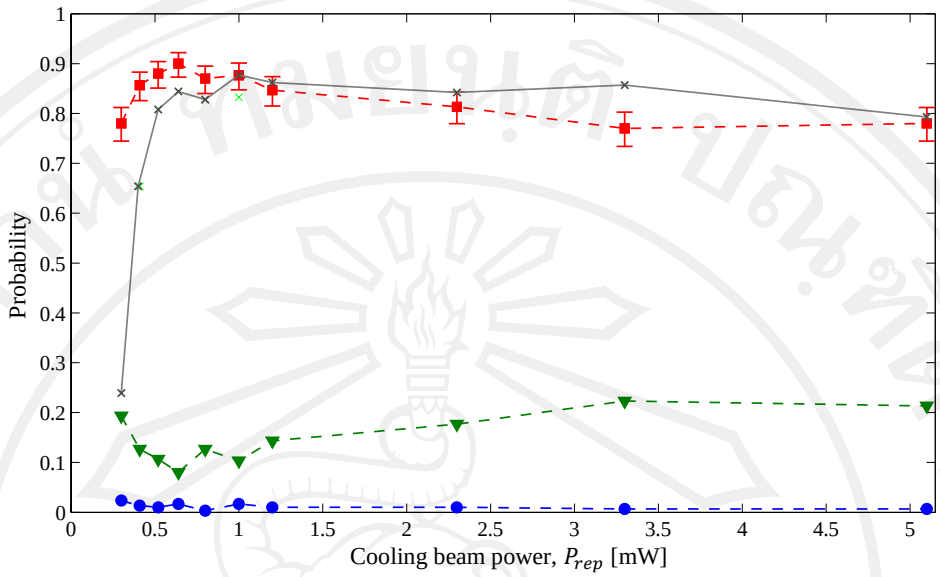

Figure 5.19. Single atom loading efficiency plotted as a function of $\boldsymbol{P_{rep}}$.

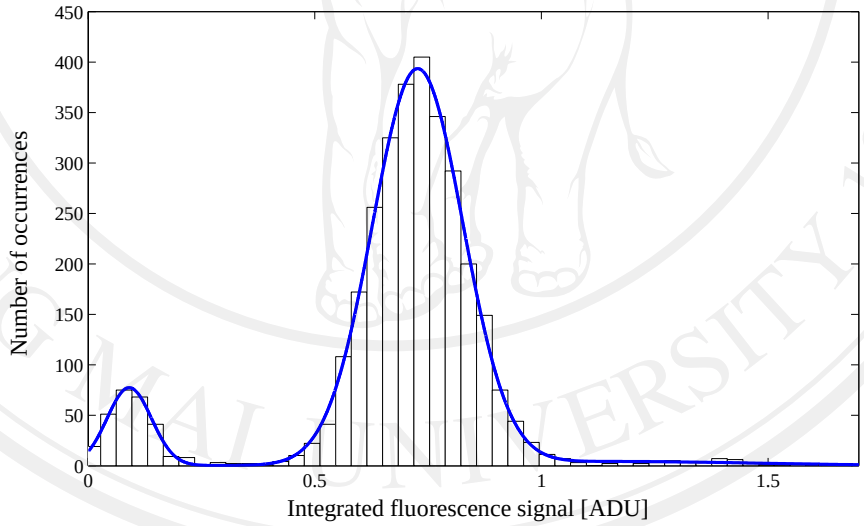

Figure 5.20. Histogram of the integrated fluorescence signal of each image for 3200 realizations of single atom preparation where the parameters of the collision light pulse were the same parameters as used in **Figure 5.14**. The large peak represents the single atom loading probability of 91.000 ± 0.006%.

single atoms. For the case of high collision power, the efficiency was reduced as a result of the short lifetime.

Finally, the effect of cooling/repumping beam power on the single atom loading efficiency was investigated. In the experiment, the collision beam parameters and the cooling/repump beam detuning were fixed at the same values used in Figure 5.14 while the cooling/repump beam power was varied from 0.3 mW to 5.1 mW. For the result, the single atom loading efficiency is plotted as a function of P_{rep} as shown in Figure 5.19. The single atom lifetime substantially depends on P_{rep}. When P_{rep} increased, the single atom survival probability for 3.5 s rises up rapidly. The longer trapping lifetime leads to the higher single atom loading efficiency as shown. However, a growth of the survival probability begins to be saturated at the power of 0.64 mW where the loading efficiency is highest. For the higher power, the loading efficiency is reduced gradually due to an increase of the pair loss induced by the intense beams.

As reported above, the effect of the parameters, which were δ_{col}, P_{col}, δ_{rep}, P_{rep} and the pulse duration, on the collisions was studied for enhancing the single atom loading efficiency. The highest observed efficiency is represented in Figure 5.20. The occurrence number of integrated fluorescence signals of 3200 experimental realizations is plotted as a histogram. The largest peak of the histogram indicates the single atom loading efficiency of 91%, which is significantly increased from the previous work [21].

The unsuccessful of 9% of loading single atoms would come from the reasons as following. First, the simulation of the time evolution of the pair in Figure 5.14 predicts that the unsuccessful of 3.6% would come from the pair loss events induced by the collision beam (where $P(0|2) = 0.04$). The pair loss events happened because of the collision between two atoms with high total energy. Second, during the collision duration the cooling/repump beams also induced the pair loss with the high $P(0|2)$ of 0.96 where the pair decay time was about 4 s (see Figure 5.3). From simulation, this contributed about 1.7% unsuccessful. Third, the imperfection of the vacuum system contributes about 1.5% because of the measured single atom lifetime is about 22 s. This was estimated by using Monte Carlo simulation [21]. Fourth, the imaging system had a detection efficiency of 99.5% that leaded to about 0.5% of single atom lost during the imaging process. The last, the remaining contribution could come from an inelastic collision that the collision partners were excited in to the undesigned state (the $F' = 2$ state). In this case, the atoms would gain the energy of $h \times 362$ MHz, which is the different energy between the two excited state. This amount of energy is high enough to make both of atoms escaped from the trap.